



Modeling and Simulation of Mild Wear of Spur Gear Considering Radial Misalignment

Paras Kumar¹ · Harish Hirani² · Atul Kumar Agrawal¹

Received: 23 May 2016 / Accepted: 5 February 2018 / Published online: 16 February 2018
© Shiraz University 2018

Abstract

An appropriate clearance is required between mating gears for effective power transmission. In the present work, the effect of radial misalignment on mild wear of spur gear is modeled and simulated. The changes in the gear tooth contact geometry due to progressive wear have also been accounted in the model. The simulation results show that in the pinion dedendum region, pressure angle increases, while the contact pressure and wear depth decrease with increase in number of wear cycles. As far as the effect of radial misalignment is concerned, contact pressure decreases and wear depth increases with the increase in misalignment. In the pinion addendum region, pressure angle and wear depth increase with the increase in wear cycles, while the contact pressure and wear depth decrease with the increase in misalignment. The pressure angle and pitch point change from initial 20° (23rd pitch point) to 20.95° (26th pitch point) and 21.86° (28th pitch point) due to 0.5- and 1-mm radial misalignment, respectively. The wear depths after 50,000 wear cycles are $-1.32 \times 10^{-2} \mu\text{m}$, $-3.33 \times 10^{-3} \mu\text{m}$ and $-4.39 \times 10^{-4} \mu\text{m}$ at 23rd, 26th and 28th pitch points, respectively. The effect of radial misalignment on backlash, pressure angle, pitch point, contact ratio, double tooth contact region and speed ratio is also discussed.

Keywords Spur gear · Wear simulation and modeling · Progressive wear · Radial misalignment · Backlash

List of symbols

a_H	Semi-Hertzian contact width
E	Equivalent young's modulus
E_p	Young's modulus of pinion material
E_g	Young's modulus of gear material
F_t	Transmitted load
H	Hardness
K	Dimensionless wear coefficient
k	Specific wear coefficient ($= \frac{K}{H}$)
P	Contact pressure
r_A	Radius at point 'A' on involute profile
r_B	Radius at point 'B' on involute profile
S_A	Tooth thickness at point 'A' on involute profile
S_B	Tooth thickness at point 'B' on involute profile
t	Sliding duration
v	Sliding velocity

y	Distance between pitch point and the instantaneous point of contact
ω_p	Angular speed of pinion
ω_g	Angular speed of gear
φ	Pressure angle at pitch point 'P'
φ_A	Pressure angle at point 'A'
φ_B	Pressure angle at point 'B'

Subscript

p	Pinion
g	Gear

1 Introduction

Misalignment between mating gears occurs in axial, radial and angular directions. All kinds of misalignments reduce effective tooth contact area and change the load distribution between meshing gears. Manufacturing inaccuracy, assembly fault and foundation movement play a major role in increasing misalignment. Misalignment in radial direction increases backlash, vibration and noise and reduces contact along the tooth profile.

Wear of gear during tooth engagement continuously changes gear tooth profile. The material loss due to wear is

✉ Paras Kumar
paraskumar@dtu.ac.in

¹ Mechanical Engineering Department, Delhi Technological University, Delhi 110042, India

² Mechanical Engineering Department, IIT Delhi, Hauzkhaz 110016, India

non-uniform along the tooth profile due to varying rolling-sliding contact. Different wear simulation studies have been performed in the past. Archard's wear model was used to simulate mild wear of spur gear (Flodin and Andersson 1997), wear of gears with flank interference (Brauer and Andersson 2003), wear of sintered spur gear (Dhanasekaran and Gnanamoorthy 2008) and effect of wear on spur gear dynamics (Wojnarowski and Onishchenko 2003). The wear depth in Archard's wear equation is a function of specific wear coefficient, contact pressure and sliding distance or the product of sliding velocity and sliding duration. Researchers assumed different assumptions while using Archard's wear equation. Andersson and Eriksson (1990) pioneered the idea of single-point observation and assumed that contact pressure was constant during a mesh. Sliding distance between contact points was calculated by the formula proposed by Andersson (1975). Flodin and Andersson (1997) determined the contact pressure by modeling the surfaces as elastic foundation or Winkler surface. Dhanasekaran and Gnanamoorthy (2008) simulated wear in sintered spur gear under dry running condition. The sliding duration was calculated by the formula proposed by Wu and Cheng (1993). The influence of the tooth deformation and wear on spur gear dynamics was carried out both analytically and experimentally by Wojnarowski and Onishchenko (2003). Onishchenko (2008) further developed a wear model by considering the condition of machine, eccentricity of pitch circle, and instantaneous temperature and observed a considerable wear at the pitch point.

Few researchers (Lundvall and Klarbring 2001; Bajpai et al. 2004; Zhang and Liu 2015) combined finite element analysis (FEA) and Archard's wear equation to predict wear in gears. Zhang and Liu (2015) showed that the angular misalignment increased the load and accelerated surface wear. Hegadekatte et al. (2010) implemented finite element method to predict local wear in micro-gears. They found that gear tooth geometry, slip rate and line of action changed quickly after 3500 contact cycles. Patil and Kumar (2016) performed the transient structural analysis to study the effect of load, speed and lubrication on gear surface of a multi-speed gearbox.

Very few works have been seen in the literature considering backlash effect on spur gear dynamics. Backlash can make complicated influence on the dynamic behavior of the geared system. The system experiences the change from the periodic motion to chaos with increased backlash (Lu et al. 2014). Khabou et al. (2012) proposed a theoretical model to

analyze the effect of the worn bearings on the nonlinear dynamic behavior of a single-stage spur gearbox.

The present work aims to investigate the effect of radial misalignment (or backlash) on mild wear of spur gear. The effect of wear progression and radial misalignment on pressure angle, contact pressure, pressure line and pitch point is also discussed. The Archard's wear model is used to simulate mild wear along tooth profile, and the change in the gear tooth contact geometry due to progressive wear is also accounted in the wear simulation model.

2 Mathematical Modeling

2.1 Effect of Radial Misalignment on Backlash (BL)

The pinion and gear are represented by their pitch circle of diameters d_p and d_g , respectively. The contact between teeth starts where the addendum circle of the gear intersects the common tangent C_1C_2 at the base circles. The point of contact moves along common tangent C_1C_2 till the end of contact, where the addendum circle of the pinion intersects again at the common tangent C_1C_2 . If the center distance (CD) between pinion and gear CD is equal to $(d_p + d_g)/2$, the two pitch circles touch exactly at the pitch point P and constant speed ratio is obtained according to the law of gearing. If due to assembly fault or bearing play, radial misalignment increases the center distance by an amount Δy then the standard pitch circles touch at a new pitch point \bar{P} as shown in the enlarged view of Fig. 1. Two new pitch circles of radii $\bar{d}_p/2$ and $\bar{d}_g/2$ are drawn through this new pitch point \bar{P} with centers \bar{O}_1 and \bar{O}_2 , respectively, as shown in Fig. 1.

Because of the shift in base and pitch circles, the line of action shifts from C_1C_2 to $\bar{C}_1\bar{C}_2$ and alters the pitch point from P to \bar{P} . This new line of action changes the pressure angle from α to $\bar{\alpha}$ and is calculated as follows (Maitra 2012)

$$\cos \bar{\alpha} = \frac{CD}{(CD + \Delta y)} \cos \alpha \quad (1)$$

The center distance variation as a result of radial misalignment increases backlash between the mating gears, which leads to non-uniform speed variation and increased level of vibration.

The backlash between mating gears due to center distance variation is computed as

$$\text{Backlash(BL)} = \text{Circular pitch measured on new pitch circle}(\bar{p}) - \text{Sum of tooth thicknesses measured along new pitch circle}(\bar{th}_s) \quad (2)$$

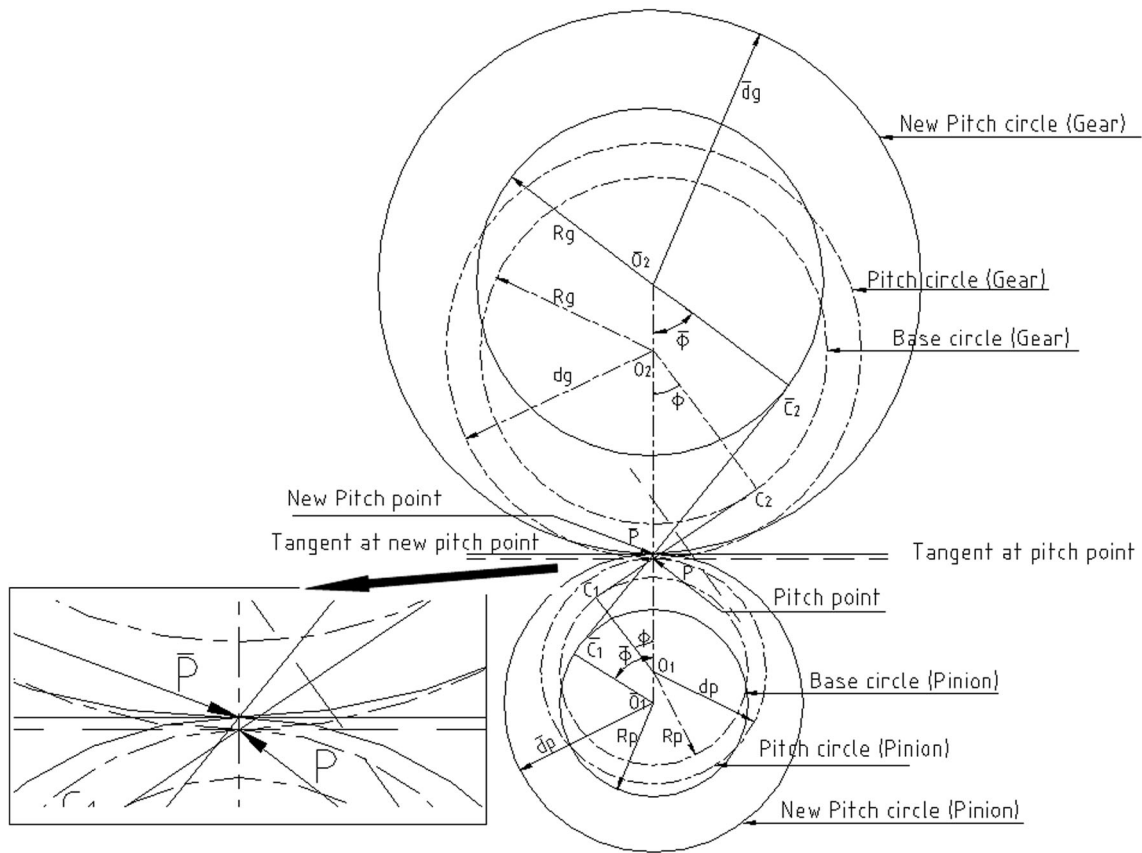


Fig. 1 Backlash effect on spur gear contact mechanics

where

$$\bar{p} = \frac{(CD + \Delta y)}{CD} \pi m \tag{3}$$

and the sum of tooth thicknesses measured is calculated as

$$\begin{aligned} \bar{th}_s &= (\bar{th}_p + \bar{th}_g) \\ &= \frac{(CD + \Delta y)}{CD} (th_p + th_g) + 2 \frac{(CD + \Delta y)}{CD} (inv\bar{\alpha} - inv\alpha) \end{aligned} \tag{4}$$

After putting the values of \bar{p} and \bar{th}_s in Eq. (2), the final expression of backlash becomes

$$\text{Backlash(BL)} = 2 \frac{(CD + \Delta y)}{CD} (inv\bar{\alpha} - inv\alpha) \tag{5}$$

The new pressure angle modifies the distances between the new pitch point and the centers of rotation of pinion and gear, thereby changing the speed ratio and contact ratio.

2.2 Effect of Wear on Tooth Thickness and Pressure Angle

As a progressive wear simulation model is proposed, the tooth contact geometry changes as a result of wear. Wear

reduces the tooth thickness and modifies pressure angle along involute profile as follows.

Suppose the two points ‘A’ and ‘B’ are considered on the involute profile as shown in Fig. 2, the relationship between their tooth thicknesses in terms of pressure angle is expressed as (Maitra 2012):

$$th_B = 2r_B \left[\frac{th_A}{2r_A} + inv\varphi_A - inv\varphi_B \right] \tag{6}$$

where th_A and φ_A are the tooth thickness and pressure angle at point ‘A’, and th_B and φ_B are the tooth thickness and pressure angle at point ‘B’.

Taking log on both sides and differentiating with respect to th_B

$$\frac{\Delta th_B}{th_B} = \frac{\Delta r_B}{r_B} + \frac{\Delta th_A}{th_A} - \frac{\Delta r_A}{r_A} + \frac{\Delta(inv\varphi_A)}{inv\varphi_A} - \frac{\Delta(inv\varphi_B)}{inv\varphi_B} \tag{7}$$

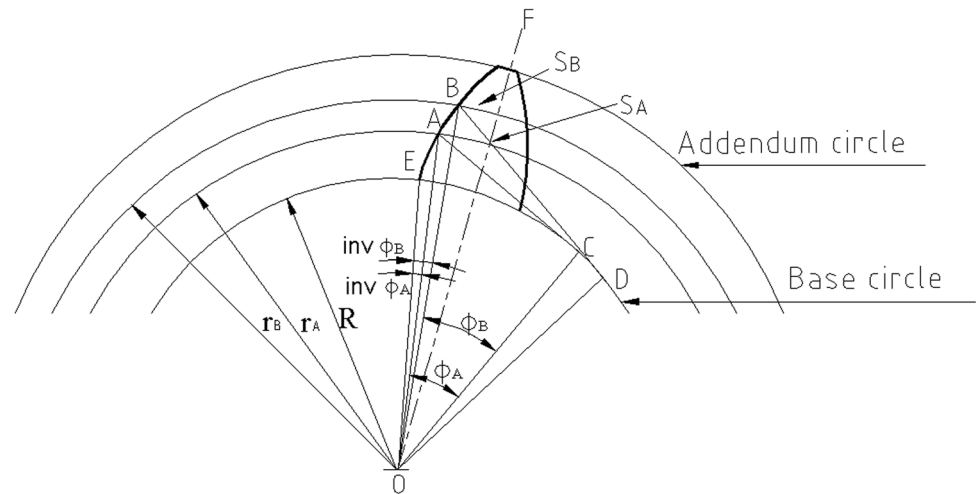
If the thickness is computed at the same radius, then $\Delta r_A = 0$ and $\Delta r_B = 0$ and Eq. (8) becomes

$$\frac{\Delta th_B}{th_B} = \frac{\Delta th_A}{th_A} + \frac{\Delta(inv\varphi_A)}{inv\varphi_A} - \frac{\Delta(inv\varphi_B)}{inv\varphi_B} \tag{8}$$

where symbol Δ represents the difference in old and new values of the parameter.

The change in tooth thickness is computed as

Fig. 2 Pressure angle and tooth thickness notation at point 'A' and 'B' on spur gear tooth



$$\Delta th(= \text{wear}) = \text{old tooth thickness}(th_0) - \text{new tooth thickness}(th_n) \quad (9)$$

and the change in pressure angle is calculated as

$$\Delta(\text{inv}\varphi) = \text{New pressure angle}(\text{inv}\varphi_n) - \text{old pressure angle}(\text{inv}\varphi_0) \quad (10)$$

If the thickness difference at any two points and difference in pressure angle at one point along involute profile are known, then the modified pressure angle is computed at the other point due to wear using Eq. (10).

The wear depth at any contact point along tooth profile is calculated using Archard's wear equation

$$\text{Wear} = kpv t \quad (11)$$

where k is the wear coefficient, p is contact pressure, v is the sliding velocity and t is the sliding duration. The complete details for calculating contact pressure, sliding velocity and sliding duration are given in "Appendix A".

A MATLAB code is written to simulate mild wear in spur gears using Archard's wear equation incorporating radial misalignment and wear effect on tooth contact geometry. To calculate the wear along tooth profile, instantaneous points of contact are considered on the involute profile. At each instantaneous point, contact pressure, sliding velocity and duration are computed. The changes in these parameters after each wear cycle are also incorporated in the model to predict the amount of material removed from the surface.

3 Simulation Scheme

The flow chart of complete simulation scheme used to obtain the wear of spur gear is shown in Fig. 3. The various steps involved in simulation are as follows:

- Input gear geometry and operating parameters, material properties and various indices like number of points on involute profile, wear cycles and radial misalignment (RM).
- Calculate addendum circle diameter, base circle diameter, pitch circle diameter and pitch line velocity.
- Calculate pressure angle, tooth thickness, distance of point of contact from pitch point, cylinder radius, contact radius, peripheral velocity, sliding velocity and sliding duration at each instantaneous point of contact. If radial misalignment index (RMI) = 1, then enter the value of RM.
- Compute semi-Hertzian contact width, contact pressure and wear depth at each point of contact.
- Recalculate tooth thickness after subtracting wear depth and pressure angle in each wear cycle. Go to step (c) until required number of wear cycles have been completed.
- Store and plot the following matrix: pressure angle, contact pressure, wear depth, pressure line variation, etc.

4 Results and Discussion

The main focus of the present work is to investigate the effect of radial misalignment (RM) on backlash, pressure angle, contact pressure, wear depth and pressure line. Wear of spur gear simulation has been performed for geometric and operating parameters as shown in Table 1. Initially the center distance between pinion and gear is maintained as 80 mm to ensure exact mating of pitch circles at pitch point P. The calculated value of backlash (BL) between the mating gears is 45.5 μm at 80-mm center distance. Later on, radial misalignment (RM) is varied by 0.5 and 1 mm, which increases the backlash from its initial value to 54.65

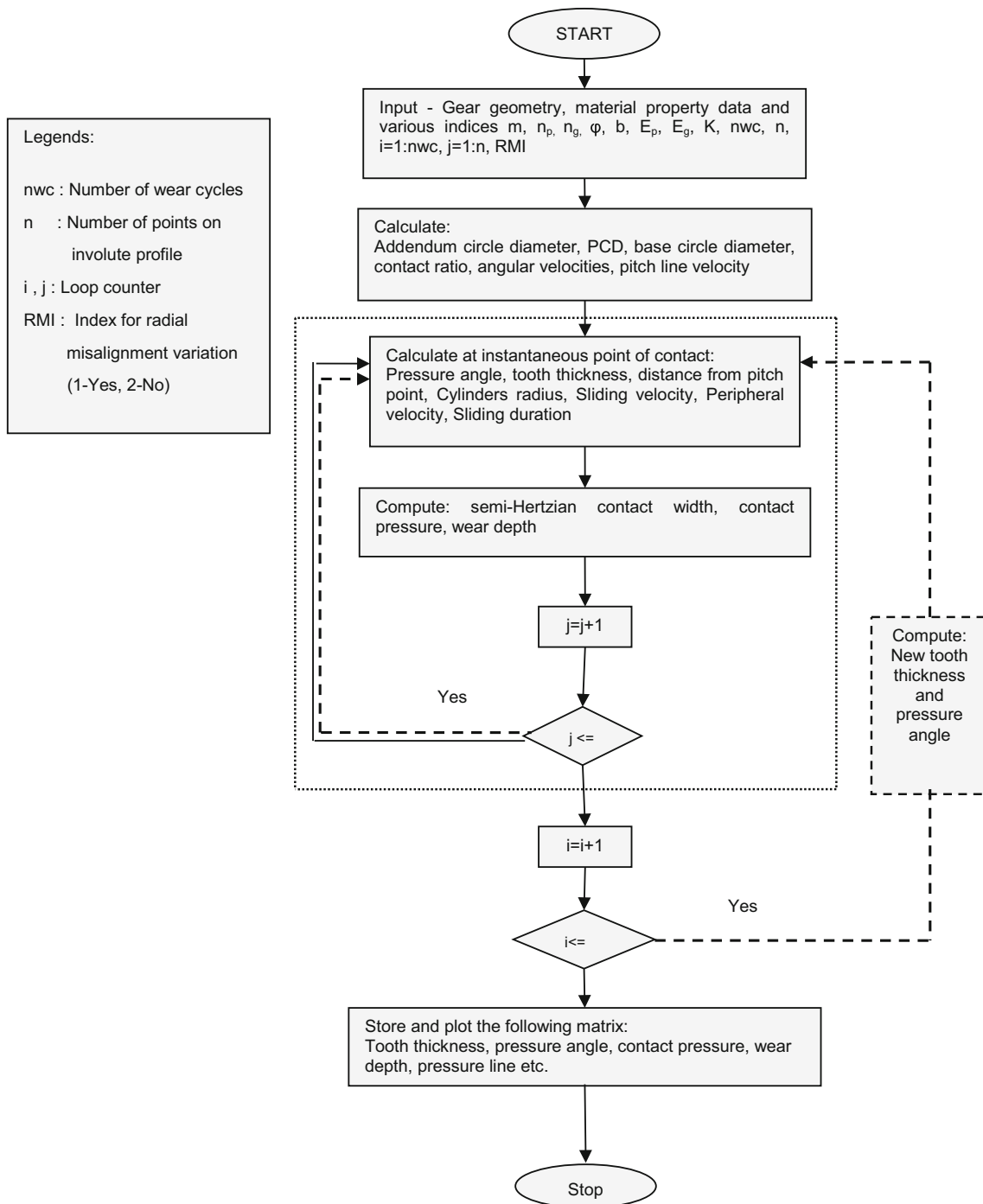


Fig. 3 Flow diagram of overall solution scheme

and 65 μm , respectively. The non-uniform wear along tooth profile changes tooth thickness, pressure angle, contact pressure and pressure line, etc. The progressive wear along tooth profile is modeled using Archard’s wear equation incorporating changes in wear-dependent parameters after each wear cycle.

The effect of number of wear cycles and radial misalignment (or backlash) on instantaneous pressure angle (IPA) of pinion is shown in Fig. 4. The pinion tooth profile is segmented into 50 instantaneous points of contact. The point number ‘1’ represents start of contact (pinion dedendum region), and the point number ‘50’ shows the

Table 1 Spur gear specifications, material properties and operating parameters

Parameters	Unit	Pinion	Gear
Number of teeth (Z)	–	27	53
Module (m)	mm	2	–
Pressure angle	Degree	20	–
Face width (w)	mm	33	–
Torque (T)	M-m	100	–
Pinion speed (N)	rpm	2000	1000
Specific wear coefficient (k)	mm ² /N	6×10^{-10}	–
Young’s modulus (E)	N/mm ²	2.1×10^5	–
Poisson’s ratio (μ)	–	0.3	–
Center distance (CD)	mm	80	–
Radial misalignment (RM)	mm	0.5, 1 mm	–

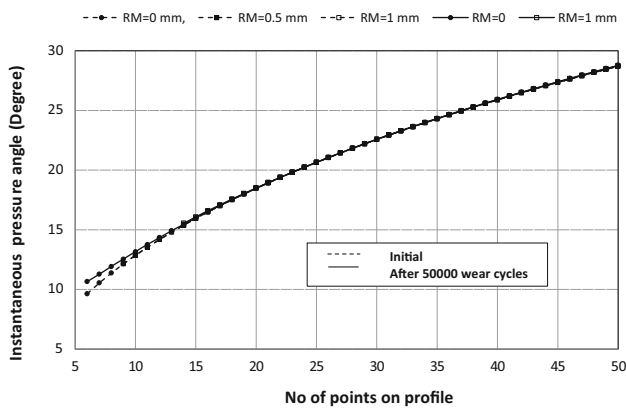


Fig. 4 Instantaneous pressure angle (IPA) variation along tooth profile

end of the contact (pinion addendum region). Instantaneous pressure angle increases with decrease in tooth thickness along tooth profile from dedendum to addendum region and attains a value of 20° at pitch point (23rd point). Not much change is observed in pressure angle with radial misalignment except the shifting of points of contact and pitch (which are overlapped in Fig. 4). The initial pitch point is shifted from 23rd contact point to 26th and 28th contact points, which increases the pressure angle from 20° to 20.95° and 21.86°, due to 0.5- and 1-mm radial misalignment, respectively. Figure 4 also shows that with increase in number of wear cycles, pressure angle increases along the tooth profile with and without radial misalignment. The maximum difference in pressure angle occurs at the start of contact in pinion dedendum region. Due to 1-mm radial misalignment, the contact between mating gears starts at 14th point of contact instead of 6th contact point initially (RM = 0). The maximum difference is 1.2° (at 6th contact point) without misalignment (RM = 0),

while 0.16° difference is observed at 14th contact point with 1-mm misalignment. The difference in pressure angle increases in dedendum region, while it decreases in addendum region with increase in radial misalignment.

The wear of pinion tooth also modifies Hertzian contact pressure as shown in Fig. 5. The highest contact pressure is observed at the lowest point of single-tooth contact (LPSTC) followed by the highest point of single-tooth contact (HPSTC). The maximum pressure in this region is attributed to the single tooth contact where the full load is shared by single-tooth pair. The start of tooth contact in pinion dedendum region also experiences higher contact pressure due to less semi-Hertzian contact width. The effect of radial misalignment is to lower the contact pressure along tooth profile. The decrease in contact pressure with increase in radial misalignment improves the contact fatigue life of the gears (Kumar et al. 2017).

The contact pressure also decreases with increase in number of wear cycles as shown in Fig. 6. The increase in semi-Hertzian contact width with wear cycles reduces contact pressure. The effect of radial misalignment on contact pressure is to decrease its value in both dedendum and addendum regions. Highest decrease in contact pressure of 31.5 MPa is observed at the starting contact point without misalignment (RM = 0).

Figure 7 shows the variation of instantaneous wear depth along tooth profile with and without radial misalignment. The wear depth in pinion dedendum region decreases with increase in number of wear cycles, and it increases with increase in misalignment. In pinion addendum region, an opposite trend is observed, i.e., wear depth increases with increase the in number of wear cycles and it decreases with the increase in misalignment. The effect of radial misalignment on cumulative wear pattern after 50,000 wear cycles is shown in Figs. 8, 9 10. Without radial misalignment (Fig. 8), wear is more on the initial contact region, while with increase in radial misalignment (Figs. 8 and 10), higher wear region shifts toward the end

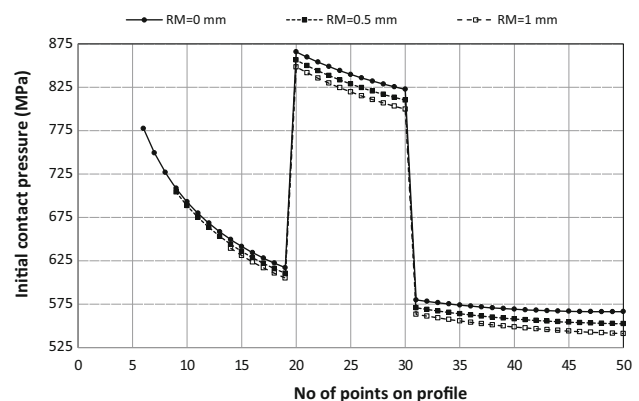


Fig. 5 Contact pressure variation along tooth profile

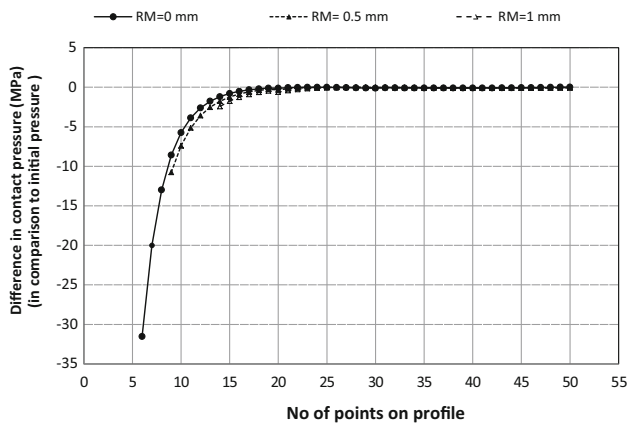


Fig. 6 Contact pressure difference due to wear and radial misalignment after 50,000 wear cycles

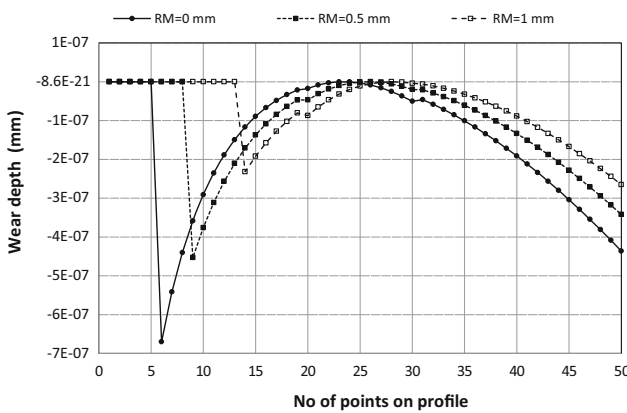


Fig. 7 Wear depth along tooth profile

of the contact in pinion addendum region. The cumulative wear pattern at pitch point also varies as shown in Fig. 11.

The initial pitch point which is at 23rd contact point (RM = 0) shifts to 26th (RM = 0.5 mm) and 28th (RM = 1 mm) points of contact due to radial

misalignment. The cumulative wear depths at 23rd, 26th and 28th pitch points after 50,000 wear cycles are $-1.32 \times 10^{-2} \mu\text{m}$, $-3.33 \times 10^{-3} \mu\text{m}$ and $-4.39 \times 10^{-4} \mu\text{m}$, respectively. According to Archard’s equation, wear depth at the pitch point is zero due to zero sliding velocity or pure rolling motion. This shifting to the new pitch point due to radial misalignment causes some relative sliding velocity at old pitch point, which contributes to small wear at old and new pitch points. Similar findings were reported in the literature experimentally (Wojnarowski and Onishchenko 2003; Onishchenko 2008), where wear occurred at pitch point due to center distance variation.

The force is transmitted from driver gear to the driven gear along the pressure line. It makes a constant pressure angle with common tangent at pitch point for involute profile. The line of action also varies with radial misalignment and wear as shown in Fig. 12. As observed in Fig. 1, due to radial misalignment, pressure line passes through a new pitch point \bar{P} instead of P. Similar type of trend is observed in wear simulation results as shown in Fig. 12, where higher misalignment/backlash shows more deviation in pressure line. This pressure line variation causes pressure angle to change from 20° to 20.95° and 21.86° due to 0.5- and 1-mm radial misalignment, respectively. Slight change in pressure angle is also observed due to wear of tooth profile.

The decreases in path of contact, contact ratio and speed ratio are shown in Table 2. The percentage decrease in contact ratio is 11.7 and 29.5% due to 0.5- and 1-mm radial misalignment. Small change in speed ratio is also observed due to misalignment. The shifting of initial point of contact (or increase in non contact region) from 6th to 14th point of contact due to 1-mm radial misalignment decreases double tooth contact region by 29.5%.

Fig. 8 Wear pattern after 50,000 wear cycles without radial misalignment

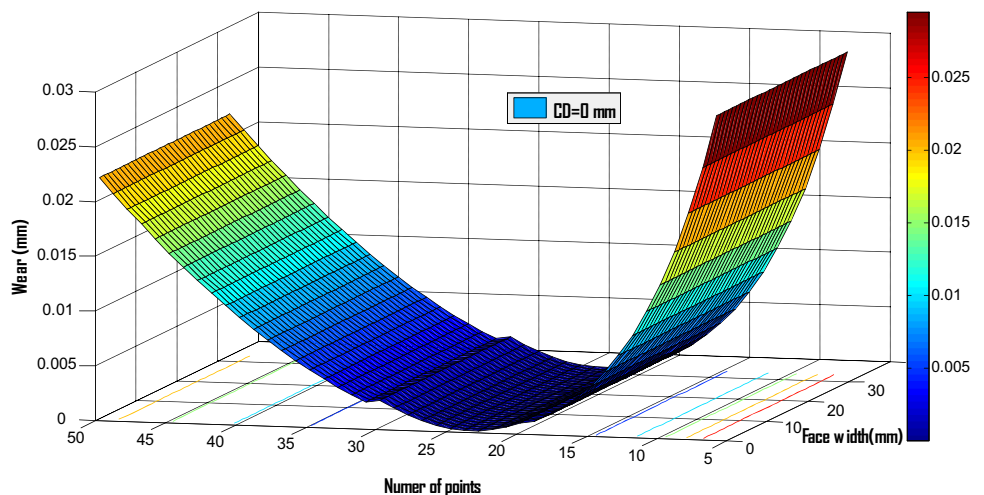


Fig. 9 Wear pattern after 50,000 wear cycles at 0.5-mm radial misalignment

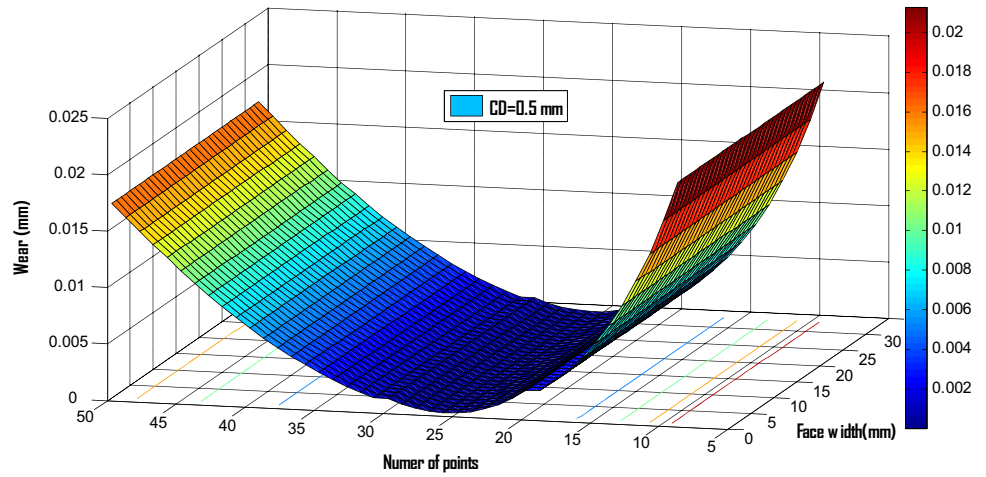


Fig. 10 Wear pattern after 50,000 wear cycles at 1.0-mm radial misalignment

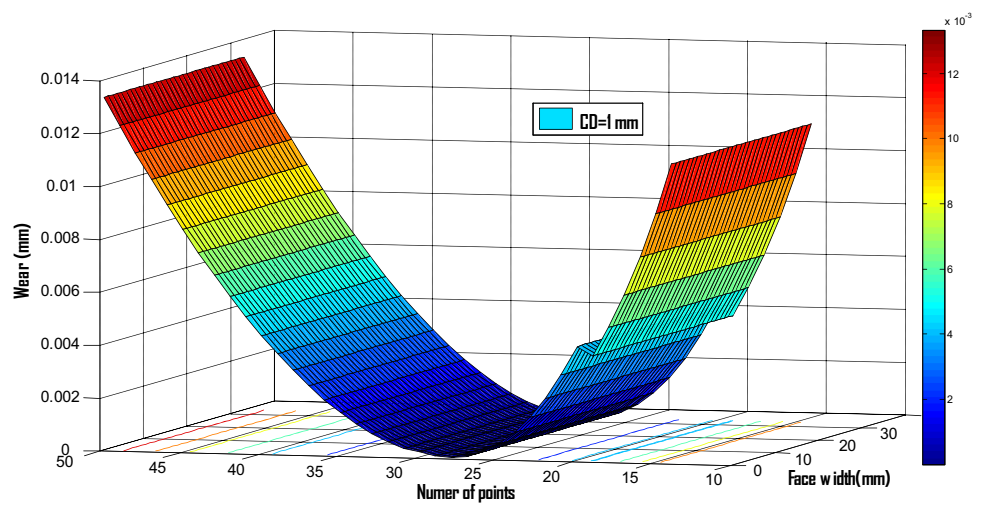


Fig. 11 Cumulative wear at pitch points (23rd, 26th and 28th) after 50,000 wear cycles

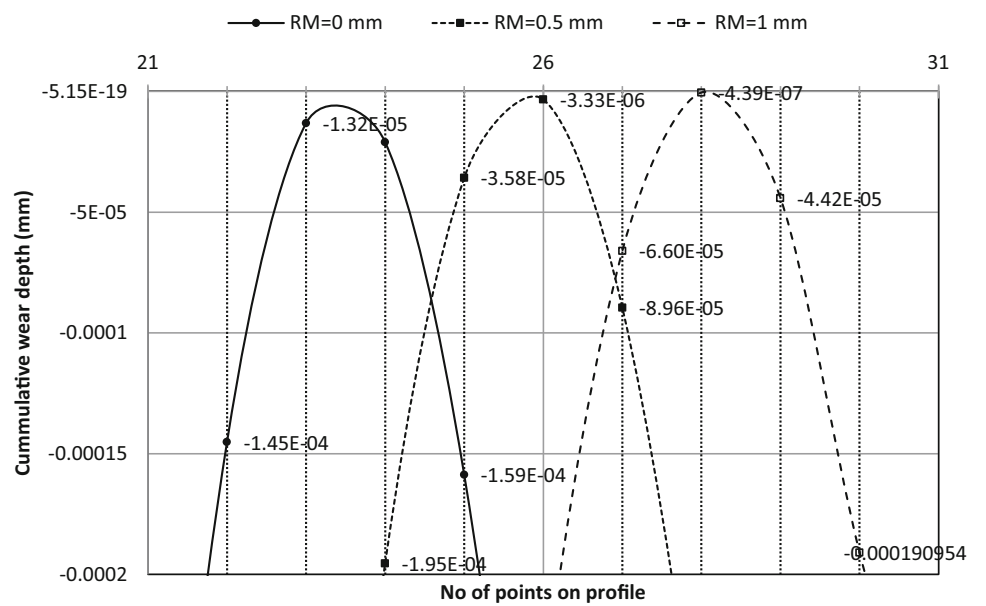


Fig. 12 Pressure line variation

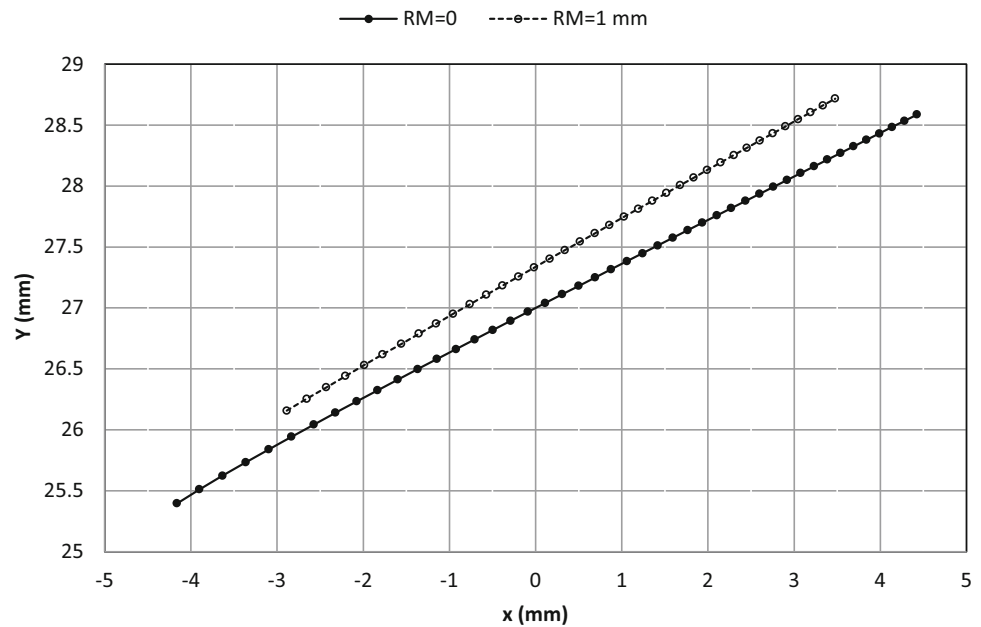


Table 2 Variation in spur gear parameters due to center distance variation

S. No	Center distance variation (CD) (mm)	Working pressure angle (α) (Degree)	Circular pitch (P_c) (mm)	Path of contact (PC) (mm)	Contact ratio (CR) –	Speed ratio $\left(\frac{\omega_p}{\omega_g}\right)$ –
1	0	20.00	6.28	10.02	1.7	1.963
2	0.5	20.95	6.32	8.59	1.5	1.961
3	1.0	21.86	6.36	7.22	1.2	1.959

5 Conclusion

The prime objective of this research is to analyze the effect of radial misalignment on wear behavior of mating spur gears. A progressive wear simulation model is proposed based on Archard’s wear equation. The change in pressure angle, contact pressure, pressure line and variation in pitch point are also discussed. The following salient points are concluded from the present study.

- Radial misalignment (RM) increases backlash and shifts pitch point to a new position. The pressure angle also changes from its initial value of 20° to 20.95° and 21.86° due to 0.5- and 1-mm radial misalignment, respectively. The effect of wear is to increase the pressure angle, and the maximum variation occurs in dedendum region of pinion.

- Hertzian contact pressure decreases due to radial misalignment and number of wear cycles. The highest contact pressure is observed at lowest point of single-tooth contact (LPSTC) followed by highest point of single-tooth contact (HPSTC).
- Due to pitch point variation, cumulative wear is observed along tooth profile including initial pitch point (23rd) and new pitch points (26th and 28th). The cumulative wear depths after 50,000 wear cycles at 23rd, 26th and 28th pitch points are $-1.32 \times 10^{-2} \mu\text{m}$, $-3.33 \times 10^{-3} \mu\text{m}$ and $-4.39 \times 10^{-4} \mu\text{m}$, respectively.
- Transmission error occurs due to pressure line variation, and the speed ratio decreases from 1.963 to 1.959 due to 1-mm radial misalignment. The initial contact point between mating gears shifts from 6th to 14th point of contact due to 1-mm radial misalignment and reduces double tooth contact region by 29.5%.

Appendix A

S. No. (Eq. No)	Parameter	Formula to compute wear depth		References
		Pinion	Gear	
A 1.	Semi-Hertzian pressure	$p = \frac{2F_t}{\pi a_H^2} \sqrt{(a_H^2 - x^2)}$		Flodin and Andersson (1997)
A 2.	Peripheral velocity	$v_p = \omega_p r_p$	$v_g = \omega_g r_g$	
A 3.	Sliding velocity	$v = (\omega_p + \omega_g)y$		
A 4.	Sliding duration	$t = \left(\frac{1}{u_p}\right) \sec \phi y$		Wu and Cheng (1993)
A 5.	Semi-Hertzian contact width	$a_H = \sqrt{\frac{AF_t E}{\pi R}}$		Flodin and Andersson (1997)
A 6.	Cylinder radius	$r_p = \frac{d_p}{2} \sin \phi + y$	$r_g = \frac{d_g}{2} \sin \phi + y$	Wu and Cheng (1993)
A 7.	Equivalent radius	$\frac{1}{R} = \frac{1}{r_p} + \frac{1}{r_g}$		Flodin and Andersson (1997)
A 8.	Equivalent young's modulus	$\frac{1}{E} = \frac{(1-\nu_p^2)}{E_p} + \frac{(1-\nu_g^2)}{E_g}$		

References

- Anderson S, Eriksson B (1990) Prediction of the sliding wear of spur gears. In: Proceedings of Nordtrib'90, Hirthshals, Denmark
- Andersson S (1975) Partial EHD theory and initial wear of gears. Doctoral Thesis, Royal Institute of Technology, Stockholm
- Bajpai P, Kahraman A, Anderson NE (2004) A surface wear prediction methodology for parallel-axis gear pairs. *J Tribol* 126:597–605
- Brauer J, Andersson S (2003) Simulation of wear in gears with flank interference—a mixed FE and analytical approach. *Wear* 254:1216–1232
- Dhanasekaran S, Gnanamoorthy R (2008) Gear tooth wear in sintered spur gears under dry running conditions. *Wear* 265:81–87
- Flodin A, Andersson S (1997) Simulation of mild wear in spur gears. *Wear* 207:16–23
- Hegadekatte V, Hilgert J, Kraft O, Huber N (2010) Multi time scale simulations for wear prediction in micro-gears. *Wear* 268:316–324
- Khabou MT, Hentati T, Abbes MS, Chaari F, Haddar M (2012) Nonlinear modeling and simulation of spur gear with defected bearings. *Multidiscip Model Mater Struct* 8(2):97–212
- Kumar P, Hirani H, Agrawal AK (2017) Fatigue failure prediction in spur gear pair using AGMA approach. *Mater Today: Proc* 4:2470–2477
- Lu JW, Chen H, Zeng FL, Vakakis AF, Bergman LA (2014) Influence of system parameters on dynamic behavior of gear pair with stochastic backlash. *Meccanica* 49:429–440
- Lundvall O, Klarbring A (2001) Simulation of wear by use of a non-smooth Newton method—a spur gear application. *Mech Struct Mach* 29(2):223–238
- Maitra GM (2012) Handbook of gear design. Tata McGraw Hill, New Delhi
- Onishchenko V (2008) Tooth Wear modeling and prognostication parameters of engagement of spur gear power transmissions. *Mech Mach Theory* 43:1639–1664
- Patil P, Kumar A (2017) Dynamic structural and thermal characteristics analysis of oil-lubricated multi-speed transmission gearbox: variation of load, rotational speed and convection heat transfer. *Iran J Sci Technol Trans Mech Eng* 41(4):281–291
- Wojnarowski J, Onishchenko V (2003) Tooth wear effects on spur gear dynamics. *Mech Mach Theory* 38:161–178
- Wu S, Cheng HS (1993) Sliding wear calculation in spur gears. *J Tribol* 115:493–500
- Zhang J, Liu X (2015) Effects of misalignment on surface wear of spur gears. *Proc I Mech E Part J: J Eng Tribol* 229(9):1145–1158